

Efficient Maximum Likelihood DOA Estimation for Signals with Known Waveforms in the Presence of Multipath

Mats Cedervall and Randolph L. Moses

Abstract—We present a large-sample maximum likelihood (ML) algorithm for estimating the directions of arrival (DOA's) and signal amplitudes of known, possibly coherent signals impinging on an array of sensors. The algorithm is an extension of the DEML method of Li *et al.* that handles coherent multipath that may be present in the signals. The algorithm is computationally efficient because the nonlinear minimization step decouples into a set of minimizations of smaller dimension.

I. INTRODUCTION

Array signal processing has been a topic of considerable interest. A number of high-resolution DOA estimation algorithms have been developed, including MUSIC, ESPRIT, and MODE. (see, e.g., [4], [5], [7], and the references therein). There have also been considerable developments on the accuracy of these techniques (see, e.g., [6]).

More recently, there has been interest in developing algorithms that assume some *a priori* signal knowledge to improve DOA estimation capability [1], [2]. This interest is motivated by applications in which partial knowledge of the incoming signals is a reasonable assumption. One such application is mobile telecommunications, where incoming signals of interest have known preamble sequences that can be exploited to improve DOA estimation accuracy and/or decrease computational cost.

One attractive algorithm for DOA estimation of known signals is the decoupled maximum likelihood (DEML) method [2]. The DEML method is a large sample ML algorithm that is computationally efficient because the nonlinear minimization step in the algorithm decouples into a set of 1-D minimizations. The DEML algorithm in [2] is based on the assumption that the desired signals are uncorrelated with one another, and the algorithm breaks down when the signals are strongly correlated. In this correspondence, we extend the DEML algorithm to handle coherent signals impinging on the array. The modification, which we term coherent decoupled maximum likelihood (CDEML), is also a large sample ML algorithm, and its nonlinear minimization step also decouples into a set of minimizations of smaller dimension.

II. SIGNAL MODEL AND PROBLEM FORMULATION

The array output vector $\mathbf{x}(t)$ is modeled as

$$\mathbf{x}(t) = \mathbf{A}(\boldsymbol{\theta})\mathbf{s}(t) + \mathbf{n}(t) \quad (1)$$

where $\mathbf{x}(t) \in \mathbb{C}^{m \times 1}$ is the received data vector, $\mathbf{s}(t) \in \mathbb{C}^{d \times 1}$ is the incident signal vector, and $\mathbf{n}(t) \in \mathbb{C}^{m \times 1}$ is an additive noise vector term. The matrix $\mathbf{A}(\boldsymbol{\theta})$ ($m \times d$) is the array manifold describing the array transfer response as a function of the signal parameter vector

Manuscript received June 19, 1995; revised August 11, 1996. This work was supported by a grant from the Swedish Institute, by NUTEK under Project 93-03103, and by the U.S. Army Research Laboratory under Contract DAAL01-93-C-0095. The associate editor coordinating the review of this paper and approving it for publication was Prof. Hagit Messer-Yaron.

M. Cedervall is with Systems and Control Group, Department of Technology, Uppsala University, Uppsala, Sweden.

R. L. Moses is with the Department of Electrical Engineering, The Ohio State University, Columbus, OH 43210 USA.

Publisher Item Identifier S 1053-587X(97)01884-9.

$\boldsymbol{\theta} = [\theta_1, \theta_2, \dots, \theta_d] \in \mathcal{R}^{d \times 1}$. Each column of $\mathbf{A}(\boldsymbol{\theta})$ is a steering vector $\mathbf{a}(\theta_k)$.

We make the following assumptions in the derivation of the algorithm.

Assumption 1: The array manifold $\mathbf{A}(\boldsymbol{\theta})$ is unambiguous, i.e., the vectors $\{\mathbf{a}(\theta_1), \dots, \mathbf{a}(\theta_{m-1})\}$ are linearly independent for any set of distinct $\{\theta_1, \dots, \theta_{m-1}\}$. \square

Assumption 2: The noise $\mathbf{n}(t)$ is circularly symmetric zero-mean Gaussian with second-order moments

$$\begin{aligned} E[\mathbf{n}(t)\mathbf{n}^*(s)] &= \mathbf{Q}\delta_{t,s} \\ E[\mathbf{n}(t)\mathbf{n}^T(s)] &= \mathbf{0} \end{aligned} \quad (2)$$

where $(\cdot)^*$ denotes complex conjugate transpose. The noise covariance matrix \mathbf{Q} is assumed to be positive definite but is otherwise unknown. \square

Assumption 3: The impinging signals $\mathbf{s}(t)$ are scaled versions of a set of c known sequences $\{y_1(t), \dots, y_c(t)\}$. In other words

$$\mathbf{s}(t) = \mathbf{F}\mathbf{y}(t) \quad (3)$$

where $\mathbf{y}(t) = [y_1(t), \dots, y_c(t)]^T$, and \mathbf{F} is a $(d \times c)$ matrix. The source signals $y_k(t)$ are assumed to be “quasistationary” [3], that is, the “covariance matrix” of $\mathbf{y}(t)$ given by

$$\mathbf{R}_{yy} = \lim_{N \rightarrow \infty} \frac{1}{N} \sum_{t=1}^N \mathbf{y}(t)\mathbf{y}^*(t) \quad (4)$$

is well defined. We assume $\mathbf{R}_{yy} > 0$ and that the source signals and noise vectors are uncorrelated so that $\mathbf{R}_{yn} = \mathbf{0}$, with \mathbf{R}_{yn} defined similarly to \mathbf{R}_{yy} . \square

Assumption 4: The matrix \mathbf{F} in (3) has the following structure:

$$\mathbf{F} = \begin{bmatrix} \gamma_{11} & \cdots & \gamma_{1d_1} & 0 & \cdots & \cdots & 0 \\ 0 & \cdots & 0 & \gamma_{21} & \cdots & \gamma_{2d_2} & 0 & \cdots & 0 \\ \vdots & & & & \ddots & & & \ddots & \\ 0 & & \cdots & & & 0 & \gamma_{c1} & \cdots & \gamma_{cd_c} \end{bmatrix}^T \quad (5)$$

Each index $\{d_k\}_{k=1}^c$ denotes the (known) number of incoming signals corresponding to the k th source signal $y_k(t)$. \square

Since there are only d unknown elements of \mathbf{F} , we parameterize \mathbf{F} as $\mathbf{F}(\boldsymbol{\gamma})$, where the $(d \times 1)$ vector $\boldsymbol{\gamma}$ is defined as

$$\boldsymbol{\gamma} = [\gamma_1^T, \gamma_2^T, \dots, \gamma_c^T]^T, \quad (d \times 1) \quad (6)$$

and where each $\gamma_k^T = [\gamma_{k1}, \dots, \gamma_{kd_k}]$. We correspondingly partition $\boldsymbol{\theta}$ as

$$\boldsymbol{\theta} = [\boldsymbol{\theta}_1^T, \boldsymbol{\theta}_2^T, \dots, \boldsymbol{\theta}_c^T] \quad (7)$$

where each $\boldsymbol{\theta}_k^T = [\theta_{k1}, \dots, \theta_{kd_k}]^T$. Thus, each incident signal $s_{kl}(t) = \gamma_{kl}y_k(t)$ and arrives at angle θ_{kl} for $k = 1, \dots, c$ and $l = 1, \dots, d_k$. The case $d_k > 1$ corresponds to coherent multipath from the $y_k(t)$ source.

The CDEML algorithm we present is derived for signal scenarios satisfying Assumptions 1–4. The DEML algorithm in [2] is a special case, imposing the additional assumption that \mathbf{F} is square and diagonal or, equivalently, that $d_k \equiv 1$. Both CDEML and DEML are large sample ML estimators when \mathbf{R}_{yy} is diagonal.

III. DERIVATION OF THE ALGORITHM

In this section, we derive a large-sample maximum likelihood (ML) estimator for θ and γ . The negative log-likelihood function of the array output vectors $\mathbf{x}(t)$, $t = 1, \dots, N$; to within an additive constant it is given by

$$L(\theta, \gamma, \mathbf{Q}) = -\ln |\mathbf{Q}| + \text{tr} \left\{ \mathbf{Q}^{-1} \frac{1}{N} \sum_{t=1}^N [\mathbf{x}(t) - \mathbf{B}\mathbf{y}(t)][\mathbf{x}(t) - \mathbf{B}\mathbf{y}(t)]^* \right\} \quad (8)$$

where $|\cdot|$ denotes the determinant of a matrix, and $\mathbf{B}(\theta, \gamma) \triangleq \mathbf{A}(\theta)\mathbf{F}(\gamma)$. In the following, we suppress the explicit dependence of \mathbf{A} , \mathbf{B} , and \mathbf{F} on θ and γ to simplify notation. An extension to the derivation in [2] shows that minimizing (8) is asymptotically equivalent to minimizing

$$F_2(\theta, \gamma) = \text{tr} [\mathbf{R}_{yy}(\mathbf{B} - \hat{\mathbf{B}})^* \hat{\mathbf{Q}}^{-1}(\mathbf{B} - \hat{\mathbf{B}})] \quad (9)$$

where $\hat{\mathbf{Q}} = \hat{\mathbf{R}}_{xx} - \hat{\mathbf{R}}_{yx} \hat{\mathbf{R}}_{yy}^{-1} \hat{\mathbf{R}}_{yx}^*$, $\hat{\mathbf{B}} = \hat{\mathbf{R}}_{yx} \hat{\mathbf{R}}_{yy}^{-1}$, $\hat{\mathbf{R}}_{yy} = 1/N \sum_{t=1}^N \mathbf{y}(t)\mathbf{y}(t)^*$, and $\hat{\mathbf{R}}_{xx}$ and $\hat{\mathbf{R}}_{yx}$ similarly defined. Equation (9) is a large sample ML estimator for a general \mathbf{R}_{yy} matrix and involves a nonlinear minimization of dimension $2d$. If we further assume that \mathbf{R}_{yy} is diagonal, which is a common situation in communications, the minimization of (9) decouples into the c minimization problems

$$\hat{\theta}_k, \gamma_k = \arg \min_{\theta_k, \gamma_k} [A(\theta_k)\gamma_k - \hat{\mathbf{b}}_k]^* \hat{\mathbf{Q}}^{-1} [A(\theta_k)\gamma_k - \hat{\mathbf{b}}_k] \quad (10)$$

$k = 1, \dots, c$

where $\hat{\mathbf{b}}_k$ denotes the k th column of $\hat{\mathbf{B}}$, and $A(\theta_k)$ is the part of \mathbf{A} corresponding to θ_k . The minimization with respect to γ_k is

$$\gamma_k(\theta_k) = \{\hat{\mathbf{Q}}^{-1/2} A(\theta_k)\}^\dagger \hat{\mathbf{Q}}^{-1/2} \hat{\mathbf{b}}_k \quad (11)$$

where $(\cdot)^\dagger$ is the Moore–Penrose pseudo inverse of a matrix. Substituting (11) into (10), we arrive at the following cost function for estimating $\hat{\theta}_k$:

$$\hat{\theta}_k = \arg \min_{\theta_k} \{\hat{\mathbf{b}}_k^* [\hat{\mathbf{Q}}^{-1} - \hat{\mathbf{Q}}^{-1} A(\theta_k) (A^*(\theta_k) \hat{\mathbf{Q}}^{-1} A(\theta_k))^{-1} A^*(\theta_k) \hat{\mathbf{Q}}^{-1}] \hat{\mathbf{b}}_k\}. \quad (12)$$

Once $\hat{\theta}_k$ is found from (12), the amplitude estimates γ_k are obtained from (11).

We remark that the above algorithm is consistent; this follows from the consistency of the exact ML and the asymptotic equivalence of the CDEML and ML methods.

Most iterative minimization algorithms require an initial estimate of the parameter vector. A simple and effective initial estimate can be found by considering the 1-D function

$$f(\theta) = \hat{\mathbf{b}}_k^* \left[\hat{\mathbf{Q}}^{-1} - \frac{\hat{\mathbf{Q}}^{-1} \mathbf{a}(\theta) \mathbf{a}^*(\theta) \hat{\mathbf{Q}}^{-1}}{\mathbf{a}^*(\theta) \hat{\mathbf{Q}}^{-1} \mathbf{a}(\theta)} \right] \hat{\mathbf{b}}_k. \quad (13)$$

The d_k values of θ giving the lowest local minima of $f(\theta)$ can then be used as the initial estimate of $\hat{\theta}_k$. This 1-D cost function is similar to a spectral MUSIC estimator for DOA's. Note also that for $d_k = 1$, $f(\theta)$ is exactly the function to be minimized in (12).

For uniform linear arrays (ULA's), i.e., arrays with uniformly spaced identical sensors, the d_k -dimensional search in (12) can be reduced to a polynomial root-finding operation using a technique similar to that developed in [7].

IV. STATISTICAL ANALYSIS

In this section, we state some results on the statistical properties of the CDEML algorithm. The asymptotic statistical properties of the parameter estimates are stated in Theorem 1. Theorem 2 gives the CRB for the corresponding signal model. Theorem 3 states that the CDEML algorithm is asymptotically efficient for diagonal \mathbf{R}_{yy} . The proofs of the theorems in this section are generalizations of the corresponding proofs in [2], and for the sake of brevity, they are omitted here. Let us define the $(3d \times 1)$ vector of real coefficients to be estimated as

$$\alpha = [\theta^T \quad \text{Re}\{\gamma^T\} \quad \text{Im}\{\gamma^T\}]^T. \quad (14)$$

Theorem 1: If \mathbf{R}_{yy} is diagonal, then the normalized asymptotic (large N) covariance matrix of $\hat{\alpha}$ is given by

$$\text{E}((\hat{\alpha} - \alpha)(\hat{\alpha} - \alpha)^T) = \frac{1}{2N} \mathbf{H}^{-1} \mathbf{V} \mathbf{H}^{-1} \quad (15)$$

$$\mathbf{H} = \begin{bmatrix} \text{Re}(\mathbf{H}_1) & \text{Re}(\mathbf{H}_2^T) & \text{Im}(\mathbf{H}_2^T) \\ \text{Re}(\mathbf{H}_2) & \text{Re}(\mathbf{H}_3) & -\text{Im}(\mathbf{H}_3) \\ \text{Im}(\mathbf{H}_2) & \text{Im}(\mathbf{H}_3) & \text{Re}(\mathbf{H}_3) \end{bmatrix}$$

$$\mathbf{V} = \begin{bmatrix} \text{Re}(\mathbf{V}_1) & \text{Re}(\mathbf{V}_2^T) & \text{Im}(\mathbf{V}_2^T) \\ \text{Re}(\mathbf{V}_2) & \text{Re}(\mathbf{V}_3) & -\text{Im}(\mathbf{V}_3) \\ \text{Im}(\mathbf{V}_2) & \text{Im}(\mathbf{V}_3) & \text{Re}(\mathbf{V}_3) \end{bmatrix}$$

$$\mathbf{H}_1 = \mathbf{D}^* \mathbf{Q}^{-1} \mathbf{D} \odot (\mathbf{F} \mathbf{F}^*)^T \quad \mathbf{V}_1 = \mathbf{D}^* (\mathbf{R}_{yy}^{-T} \otimes \mathbf{Q}) \mathbf{D}$$

$$\mathbf{H}_2 = \mathbf{A}^* \mathbf{Q}^{-1} \mathbf{D} \odot (\mathbf{F} \mathbf{E}_F^*)^T \quad \mathbf{V}_2 = \mathbf{D}^* (\mathbf{R}_{yy}^{-T} \otimes \mathbf{Q}) \mathbf{A}$$

$$\mathbf{H}_3 = \mathbf{A}^* \mathbf{Q}^{-1} \mathbf{A} \odot (\mathbf{E}_F \mathbf{E}_F^*)^T \quad \mathbf{V}_3 = \mathbf{A}^* (\mathbf{R}_{yy}^{-T} \otimes \mathbf{Q}) \mathbf{A}$$

$\mathbf{D} = \text{diag} \{\mathbf{Q}^{-1} \mathbf{D}_k \gamma_k\}_{k=1}^c$, $\mathbf{A} = \text{diag} \{\mathbf{Q}^{-1} \mathbf{A}_k\}_{k=1}^c$, $\mathbf{D} = [\mathbf{D}_1, \dots, \mathbf{D}_c] = [d_{11}, \dots, d_{1d_1}, \dots, d_{cd_c}]$, where $d_{kl} \triangleq \partial \mathbf{a}(\theta_{kl}) / \partial \theta_{kl}$, \mathbf{E}_F denotes a matrix of the same dimensions as \mathbf{F} in (5) but with the γ_{kl} replaced by ones, and \otimes denotes the Kronecker product.

Theorem 2: For the signal model in Section II under Assumptions 1–4, and for $\hat{\mathbf{R}}_{yy} > 0$, the CRB of α is given by

$$\text{CRB}(\alpha) = \frac{1}{2N} \begin{bmatrix} \text{Re}(\mathbf{F}_1) & \text{Re}(\mathbf{F}_2^T) & \text{Im}(\mathbf{F}_2^T) \\ \text{Re}(\mathbf{F}_2) & \text{Re}(\mathbf{F}_3) & -\text{Im}(\mathbf{F}_3) \\ \text{Im}(\mathbf{F}_2) & \text{Im}(\mathbf{F}_3) & \text{Re}(\mathbf{F}_3) \end{bmatrix}^{-1} \quad (16)$$

$$\mathbf{F}_1 = \mathbf{D}^* \mathbf{Q}^{-1} \mathbf{D} \odot (\mathbf{F} \hat{\mathbf{R}}_{yy} \mathbf{F}^*)^T$$

$$\mathbf{F}_2 = \mathbf{A}^* \mathbf{Q}^{-1} \mathbf{D} \odot (\mathbf{F} \hat{\mathbf{R}}_{yy} \mathbf{E}_F^T)^T$$

$$\mathbf{F}_3 = \mathbf{A}^* \mathbf{Q}^{-1} \mathbf{A} \odot (\mathbf{E}_F \hat{\mathbf{R}}_{yy} \mathbf{E}_F^T)^T$$

and where \mathbf{D} and \mathbf{E}_F are defined as in Theorem 1.

If \mathbf{R}_{yy} is diagonal, it can be shown that the right-hand sides of (15) and (16) are asymptotically equivalent, giving us the following theorem.

Theorem 3: When \mathbf{R}_{yy} is diagonal, the CDEML algorithm is asymptotically statistically efficient.

V. NUMERICAL EXAMPLES

We examine the performance of CDEML for a uniform linear array with 10 elements, spaced half a wavelength apart. There are two known source signals; one arrives at 5° , and the other arrives from two directions: 0° and 10° . In the simulations, the source signals are chosen as uncorrelated Gaussian sequences. Unless explicitly stated otherwise, we collect 100 snapshots ($N = 100$), and the SNR of each received signal is 0 dB. The signals are equal energy; therefore

$$\mathbf{F} = \begin{bmatrix} e^{i0.25\pi} & e^{i0.5\pi} & 0 \\ 0 & 0 & e^{i0.75\pi} \end{bmatrix}^T.$$

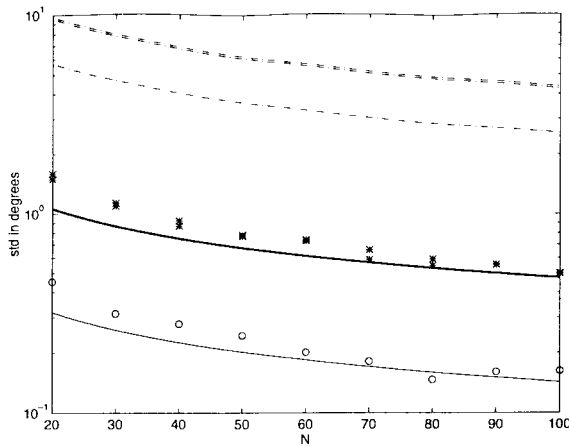


Fig. 1. CRB's for CDEML (solid lines) and unknown signals (dash-dotted lines). RMSE's (* and o) of DOA estimates for the CDEML algorithm, as a function of number of data samples N .

In the figures that follow, the "*" and "o" symbols show the root mean squared error (RMSE) of the CDEML algorithm DOA estimates from 100 Monte Carlo trials; the "*" results are for the two coherent signals, and the "o" results are for the single signal. The solid lines are the corresponding CRB's for these DOA estimates. The dash-dotted lines are the CRB's of the signals DOA's if the signals are assumed to be unknown. All RMSE and CRB values are presented as standard deviations in degrees.

Fig. 1 shows the RMSE of the DOA estimates of the CDEML algorithm for different numbers of snapshots N . The solid lines are the CRB standard deviations for the three received signals; the lowest curve is for the single source from 5° , and the two upper curves are for the multipath signals arriving at 0° and 10° . Since the sources are uncorrelated, these curves are also equal to the asymptotic variance of the CDEML algorithm. The simulations agree closely with the asymptotic theory even for short data lengths; in addition, the difference between simulation and asymptotic theory diminishes as N increases.

Fig. 2 shows the RMSE and CRB for the example considered as a function of array size m . As the array size increases, the CRB's of the two multipath signals approach the single source CRB. The array beamwidth is approximately $360/(\pi(m-1))$; therefore, the coherent signals are approximately 1.1 beamwidths apart for $m = 14$, when the CRB approaches the single-source CRB. Again, the simulation performance agrees closely with the statistical theory.

Fig. 3 illustrates the performance of the algorithm when the coherent signals have substantially different received powers. In this case, we have two source signals; one signal arrives in two directions: a strong signal (0 dB) at 0° to simulate a direct path and a weaker signal at 10° to simulate a weak multipath signal. The power of the multipath signal is varied between -50 and -10 dB with respect to the direct-path coherent signal. When the multipath source is of moderate power (-20 to -10 dB) the three-source statistical theory is accurate, and the CDEML algorithm performance agrees closely with the CRB. For a weaker multipath signal (-35 to -20 dB), the CDEML variances increase from their predicted values.

For very low signal powers of the multipath signal, Fig. 3 shows the effect of overestimating the number of signals in the model. In this region, the signal model is practically that of two uncorrelated signals because the multipath signal can be considered absent. The algorithm is thus using an incorrectly large model order (3 instead of 2). The weaker signal has variance corresponding to a completely random DOA. The stronger source RMSE approaches that of the

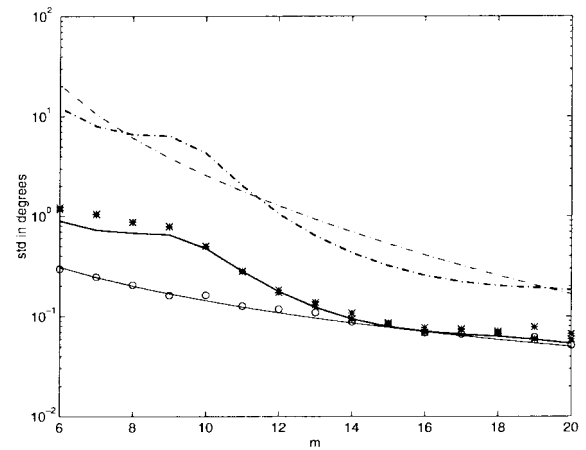


Fig. 2. CRB's for CDEML (solid lines) and unknown signals (dash-dotted lines). RMSE's (* and o) of DOA estimates for the CDEML algorithm, as a function of number of array size m .

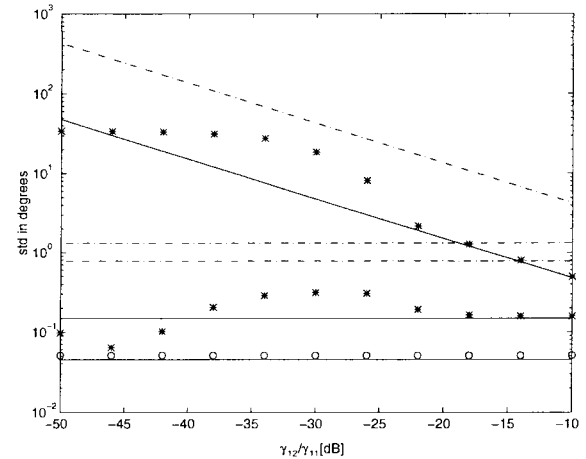


Fig. 3. CRB's for CDEML (solid lines) and unknown signals (dash-dotted lines). RMSE's (* and o) of DOA estimates for the CDEML algorithm, as a function of the ratio between the two multipath signal amplitudes (γ_{12}/γ_{11}) in dB.

CRB corresponding to a single uncorrelated signal (i.e., the lowest solid CRB line). The simulation RMSE's of the direct-path source are about 2–3 dB above this line; the increased variance results from assuming a model order that is too high for this signal environment. Simulations repeated on this case, for very weak multipath signal power values and using a model order of 2, verify that the CDEML algorithm DOA RMSE for both strong signals are close to that of the lowest solid line on the figure.

REFERENCES

- [1] J. Li and R. T. Compton, "Maximum likelihood angle estimation for signals with known waveforms," *IEEE Trans. Signal Processing*, vol. 41, pp. 2850–2862, Sept. 1993.
- [2] J. Li, B. Halder, P. Stoica, and M. Viberg, "Computationally efficient angle estimation for signals with known waveforms," *IEEE Trans. Signal Processing*, vol. 43, pp. 2154–2163, Sept. 1995.
- [3] L. Ljung, *System Identification Theory For The User*. Englewood Cliffs, NJ: Prentice-Hall, 1987.
- [4] R. Roy, A. Paulraj, and T. Kailath, "ESPRIT—A subspace rotation approach to estimation of parameters of cisoids in noise," *IEEE Trans. Acoust., Speech, Signal Processing*, vol. ASSP-34, pp. 1340–1342, Oct. 1986.
- [5] R. O. Schmidt, "Multiple emitter location and signal parameter estimation," in *Proc. RADC, Spectral Estimation Workshop*, Rome, NY, 1979, pp. 243–258.

- [6] P. Stoica and A. Nehorai, "MUSIC, maximum likelihood, and Cramér–Rao bound," *IEEE Trans. Acoust., Speech, Signal Processing*, vol. 37, pp. 720–741, May 1989.
- [7] P. Stoica and K. C. Sharman, "Maximum likelihood methods for direction-of-arrival estimation," *IEEE Trans. Acoust., Speech, Signal Processing*, vol. 38, pp. 1132–1143, July 1990.

Effect of Delay on the Performance of the Leaky LMS Adaptive Algorithm

F. Laichi, T. Aboulnasr, and W. Steenaart

Abstract—This correspondence studies the effect of a nonzero delay on the performance of the leaky LMS algorithm. The stability bound on the stepsize is derived for error convergence. It is shown that leakage allows for larger bounds on the step size of the delayed LMS algorithm. Theoretical bounds are verified by simulations.

I. INTRODUCTION

In adaptive filtering, the LMS algorithm has been widely accepted as a reasonable compromise between complexity, robustness, and speed for many applications. The basic system identification setup is given by

$$\begin{aligned} C(n) &= C(n-1) + \beta e(n)X(n), \\ e(n) &= y(n) - d(n) \end{aligned} \quad (1)$$

where

$C(n)$ coefficient vector
 $X(n)$ input vector
 $y(n)$ output value at time n
 $e(n)$ error signal defined as the difference between the output $y(n) = X^T(n)C(n-1)$ and the desired output at instant n .

In (1), the assumption is that it is possible to compute $e(n)$ fast enough to use it to update the coefficient $C(n-1)$ to obtain $C(n)$. However, this may not be feasible for a wide variety of reasons, resulting in an unavoidable delay between the availability of $d(n)$ and the corresponding update of the filter coefficients [4]. A more realistic description of the LMS algorithm is given by

$$C(n) = C(n-1) + \beta e(n-D)X(n-D). \quad (2)$$

This is the delayed LMS (DLMS) studied recently in [1]–[4]. It was shown in [1] and [2] that even though a small delay may have minimal effects on the overall performance, it definitely reduces the bound on the step size β required for the stability of the adaptive algorithm. The convergence of the algorithm was shown to be slightly slower than the LMS. As D increases, deterioration of the adaptive filter performance increases. LMS adaptation also runs into problems in other nonideal situations. Finite-precision implementations as well as spectrally insufficient inputs or feedback across the adaptive filter

Manuscript received April 23, 1994; revised June 21, 1996. The associate editor coordinating the review of this paper and approving it for publication was Dr. Virginia L. Stonick.

The authors are with the Department of Electrical Engineering, University of Ottawa, Ottawa, Ont., Canada K1N 6N5.

Publisher Item Identifier S 1053-587X(97)01891-6.

have been shown to result in "parameter drift" [7]. In this case, the filter coefficients grow without bound away from the optimum values. "Leakage" in the update equation was proven to be effective in controlling parameter drift [7]. The leaky LMS (LLMS) equation is described by

$$C(n) = (1 - \beta\mu)C(n-1) + \beta e(n)X(n). \quad (3)$$

This update equation is derived based on minimizing an augmented instantaneous square error function

$$J(n) = e(n)^2 + \mu C(n)^T C(n) \quad (4)$$

where μ is a measure of the leakage introduced. Since the norm of the coefficient vector is minimized along with the error squared, the algorithm ensures that the coefficients do not drift (depending on the value of leakage μ). This modification to the performance measure to be minimized by the adaptive filter leads to a "biased" optimum with small bias for low μ .

The delay problem discussed earlier for the LMS still exists for the LLMS. The LDLMS algorithm is given by

$$C(n) = (1 - \beta\mu)C(n-1) + \beta e(n-D)X(n-D). \quad (5)$$

In this correspondence, we will discuss the effect of the delay on the overall performance of the LLMS. First, general expressions for stability bounds and steady-state excess error formula for the leaky delayed LLMS (LDLMS) are derived. Results for regular, leaky, or DLMS are special cases of these expressions. Finally, results are confirmed through simulations.

II. CONVERGENCE OF LDLMS ALGORITHM

In this section, the convergence of the LDLMS algorithm is studied based on the mean square error. The update equation of the LDLMS is rewritten as

$$C(n) = \gamma C(n-1) + \beta e(n-D)X(n-D) \quad (6)$$

where $\gamma = 1 - \beta\mu$. Equation (6) can be reformulated in terms of coefficient error vector $\epsilon(n)$ as follows:

$$\begin{aligned} \epsilon(n) &= \gamma \epsilon(n-1) + \beta e_{opt}(n-D)X(n-D) \\ &\quad - \beta X(n-D)X(n-D)^T \epsilon(n-D-1) \\ &\quad - (1-\gamma)C_{opt} \end{aligned} \quad (7)$$

where $e_{opt}(n) = e(n) - e_{opt}$, C_{opt} is the optimum coefficient vector, and $\epsilon(n) = C(n) - C_{opt}$. Taking the expected value of both sides of (7) and using the independence assumption [6] on $X(n)$, $e_{opt}(n)$, and $\epsilon(n)$, we get

$$\begin{aligned} \langle \epsilon(n) \rangle &= \gamma \langle \epsilon(n-1) \rangle - \beta H \langle \epsilon(n-D-1) \rangle \\ &\quad - (1-\gamma)C_{opt} \end{aligned} \quad (8)$$

where H is the input correlation matrix, and $\langle \cdot \rangle$ denotes ensemble averaging. Using the standard decoupling transformation in (8)

$$\begin{aligned} H &= V \Lambda V^T \\ W(n) &= V^T (C(n) - C_{opt}) \\ &= V^T \epsilon(n) \\ U(n) &= V^T X(n) \\ R_{opt} &= V^T C_{opt} \end{aligned} \quad (9)$$

where V is an orthonormal matrix, the columns of which are the eigenvectors of H , and Λ is a diagonal matrix with the diagonal elements corresponding to the eigenvalues of H , we obtain

$$\langle W(n) \rangle = \gamma \langle W(n-1) \rangle - \beta \Lambda \langle W(n-D-1) \rangle - (1-\gamma) R_{opt}. \quad (10)$$

The first two terms on the right-hand side of (10) are a part of the natural response of the system, whereas the last term $(1-\gamma)R_{opt}$ contributes to the forced response. Considering the instantaneous cost function as [6]:

$$J(n) = J_{\min} + J_{ex}(n) = J_{\min} + \langle W(n)^T \Lambda W(n) \rangle \quad (11)$$

where J_{\min} is the minimum MSE of the LMS ($\mu = 0$ and $D = 0$), and $J_{ex}(n)$ is the excess mean-squared error at time index n . By substituting (10) into the $J_{ex}(n)$ expression in (11) and following an approach similar to that in [2], the steady-state excess MSE $J_{ex}(\infty)$ is obtained in [7] as in (12), shown at the bottom of the page, where $M = N + \nu_x - 1$, $\sigma^2 = \langle x_n^2 \rangle$, $\alpha = \sqrt{\sum \lambda_i^2 / \sum \lambda_i}$, P is the cross-correlation vector, and ϵ is the bias on the optimum tap-weight vector. This steady-state excess MSE clearly depends on μ and D . A bias term on the true optimum tap weights appears in the numerator due to the leakage parameter. This accounts for a tradeoff that has to exist between dampening the undriven adaptive tap weights and increasing the residual output error power. For $\mu = 0$, this equation is identical to [2, (c.5)] for the DLMS case.

III. LDLMS STABILITY BOUNDS ON STEP SIZE

The denominator of (12) has an infinite number of terms. However, in the region of stability, β is normally small. Hence, terms of order higher than β^4 decay quickly. The stability bound on the step size is found by determining the value of β that makes the denominator of (12) equal to zero.

$$\begin{aligned} S(\beta) \approx & 2(\sigma^2 + \mu) - \beta(2\mu\sigma^2 + \alpha M\sigma^4 + \mu^2 + 2\sigma^4 D) \\ & + \sigma^4 \beta^2 (2\mu D + \sigma^2 D(D+1)) \\ & - \beta^3 \sigma^6 D(D+1) \left(\mu + \frac{1}{3}(2D+1)\sigma^2 \right) \\ & + \beta^4 \sigma^8 D(D+1) \\ & \cdot \left[(2D+1)\mu + \frac{(D+2)(3D+1)}{6} \right] \approx 0. \end{aligned} \quad (13)$$

As β increases from zero to a value β_{\max} , $S(\beta)$ decreases monotonically from $S(0) = 2(\sigma^2 + \mu)$ to $S(\beta_{\max}) = 0$, causing $J_{ex}(\infty)$ at β_{\max} to approach infinity and, as such, drives the adaptive system to be unstable. For applications where $\beta D \ll 1$, $S(\beta)$ can be approximated as a polynomial of first order in β . In this case, $J_{ex}(\infty)$ is given by

$$J_{ex}(\infty) \cong \frac{\beta J_{\min} \alpha N \sigma^4 + \beta \mu^2 P^T H^{-1} P + 2\beta \mu \sigma^2 P^T \epsilon}{2(\sigma^2 + \mu) - \beta(2\mu\sigma^2 + \alpha M\sigma^4 + \mu^2 + 2\sigma^4 D)} \quad (14)$$

and β_{\max} is easily obtained by setting the denominator of (13) to zero. However, for moderately large values of βD , the second-order

¹ ν_x is the kurtosis of x and is defined as $\nu_x = \langle x^4 \rangle / \langle x^2 \rangle^2$

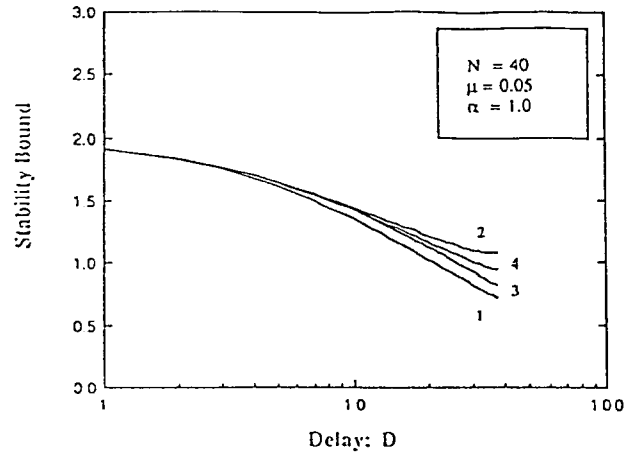


Fig. 1. Stability bounds of the LDLMS ($N\beta\sigma^2$) versus delay with $\mu = 0.05$ and $N = 40$.

term in β in (12) has to be retained. Then, the maximum step size that constitutes the upper bound on β is given by

$$\beta_{\max} = \frac{A_2 - \sqrt{A_2^2 - 4A_1A_3}}{2A_1} \quad (15)$$

where $A_1 = 2\mu D + \sigma^2 D(D+1)$, $A_2 = 2\mu\sigma^2 + \alpha M\sigma^4 + \mu^2 + 2\sigma^4 D$, and $A_3 = 2(\sigma^2 + \mu)$. For larger values of βD , if the term with third power order has to be included, numerical methods have to be employed to solve the roots of the denominator (12). Fig. 1 shows the different approximations using different powers of β for the stability bounds.

These bounds on the step size have been verified for different leakage values by computer simulations and were proven close to the theoretical ones [7]. Fig. 2 shows the approximate theoretical bound in (13) compared with the experimental ones for the LDLMS stability bound. It can be seen from Fig. 2 that as μ increases, β_{\max} increases. Table I summarizes the stability bound as a function of both delay and leakage. As expected, for $\mu = 0$, the stability bound decreases as D increases. However, as leakage is introduced ($\mu > 0$), the step-size bound for the same delay is increased, showing that leakage, in some sense, compensates for the reduction in stability bound caused by a nonzero delay. The entries in Table I are obtained by evaluating (13).

IV. SIMULATION EXAMPLES

Analysis based on LDLMS has to be employed whenever a delay in update of the adaptive algorithm is unavoidable and tap-wandering or tap-drift exists. As an illustrative example, consider the case of a system identification problem where the input does not have sufficient spectral excitation eventually leading the DLMS to drift problems. This will degrade the performance of the DLMS algorithm [1]. To counteract this parameter drift in the DLMS algorithm, the LDLMS is employed. Both the adaptive and unknown filters have the same filter length N . Fig. 3 shows the performance of the LDLMS compared with the DLMS for different values of leakage. Only one coefficient is shown as an illustrative example. The drift of the filter tap-weight for zero leakage is obvious in the figure.

$$\begin{aligned} J_{ex}(\infty) \cong & \frac{\beta J_{\min} \alpha N \sigma^4 + \beta \mu^2 P^T H^{-1} P + 2\beta \mu \sigma_x^2 P^T \epsilon}{2(\sigma_x^2 + \mu) - \beta(2\mu\sigma_x^2 + \alpha M\sigma_x^4 + \mu^2 + 2\sigma_x^4 D) + \sigma_x^4 \beta^2 (2\mu D + \sigma_x^2 D(D+1))} \\ & \cdot \frac{1}{- \beta^3 \sigma_x^6 D(D+1) \left(\mu + \frac{1}{3}(2D+1)\sigma_x^2 \right) + \beta^4 \sigma_x^8 D(D+1) \left((2D+1)\mu + \frac{(D+2)(3D+1)}{6} \right) \dots} \end{aligned} \quad (12)$$